Tumor angiogenic endothelial cell targeting by a novel integrin-targeted nanoparticle

Jianwu Xie[1]
Zhimin Shen[2]
King CP Li[1,3]
Narasimhan Danthi[1]

[1]Molecular Imaging Laboratory, Clinical Center and [2]Vaccine Research Center, National Institutes of Health, Bethesda, MD, USA; [3]Department of Radiology, The Methodist Hospital, Houston, TX, USA

Abstract: Angiogenesis is an important process in cancer growth and metastasis. During the tumor angiogenic process, endothelial cells express various cell surface receptors which can be utilized for molecular imaging and targeted drug delivery. One such protein receptor of interest is the integrin $\alpha_v\beta_3$. Our group is involved in the development of molecular imaging probes and drug delivery systems targeting $\alpha_v\beta_3$. Based on extensive lead optimization study with the integrin antagonist compounds, we have developed a new generation of integrin $\alpha_v\beta_3$ compound (IA) which has superior binding affinity to $\alpha_v\beta_3$. Utilizing this IA as a targeting agent, we have developed a novel integrin-targeted nanoparticle (ITNP) system for targeted drug delivery and imaging of cancer angiogenesis. When multiple copies of the IA were conjugated onto the nanoparticle surface, strong and selective binding to the integrin $\alpha_v\beta_3$ was observed. These ITNPs also were rapidly taken up by cells that express $\alpha_v\beta_3$. The ITNPs accumulated in the angiogenic vessels, after systemic administration in a murine squamous cell carcinoma model. This novel intergrin targeted ITNP platform will likely have an application in targeted delivery of drugs and genes in vivo and can also be used for molecular imaging.

Keywords: targeted nanoparticle, integrin $\alpha_v\beta_3$, cancer, angiogenesis

Introduction

Angiogenesis is required for cancer growth and is highly associated with cancer metastasis. Integrin $\alpha_v\beta_3$ is a cell-surface receptor protein that is upregulated in various pathological conditions including osteoporosis, rheumatoid arthritis, macular degeneration as well as cancer angiogenesis (Eliceiri and Cheresh 2000; Ruoslahti 2002). Integrin $\alpha_v\beta_3$ is a widely recognized target for the development of molecular probes for imaging angiogenesis and for cancer therapy. Integrin $\alpha_v\beta_3$ antagonists induce apoptosis on activated endothelial cells and also $\alpha_v\beta_3$ positive tumor cells (Taga et al 2002). Vitaxin, an antibody for $\alpha_v\beta_3$ and cilengitide, a cyclic peptide (Tucker 2006) both block $\alpha_v\beta_3$ and are in clinical trials as antiangiogenic agents in patients with various tumors (Gutheil et al 2000; Raguse et al 2004). A number of research groups have developed $\alpha_v\beta_3$ targeted nanomaterials for imaging and therapy (Winter et al 2003; Lim et al 2006). A paramagnetic polymerized liposomal nanoparticle was developed by attaching the $\alpha_v\beta_3$ antibody LM609 onto the surface of the nanoparticle (Storrs et al 1995), and this polymerized nanoparticle showed good tumor accumulation in the VX2 rabbit tumor model (Sipkins et al 1998). Similar targeted polymerized liposomes have also been developed for targeted gene delivery, in which the targeting agent is a small molecule integrin antagonist instead of an antibody (Hood et al 2002). These particles also demonstrated angiogenesis targeting in murine tumor models. We have developed a novel integrin antagonist which has more than 20 times better binding affinity to $\alpha_v\beta_3$ compared to the one that was used by Hood et al (Duggan et al 2000; Burnett et al 2005). Here we report a novel ITNP system that has this high affinity integrin antagonist compound as the

Correspondence: Narasimhan Danthi
Building 10 Room 1N306, 10 Center Drive, Bethesda, MD, USA
Tel +1 301 451 5170
Fax +1 301 435 2714
Email ndanthi@cc.nih.gov

targeting agent and the subsequent studies involving the in vivo tumor angiogenesis targeting.

Methods and materials

Synthesis of targeting lipid BisT-PE-EDTA-IA (Scheme 1)

Ethylenediaminetetraacetic acid dianhydride (EDTA-dianhydride, 135 mg, 525 μmoles) was dissolved in a dry 3-neck flask, under a positive pressure of argon, in pyridine (20 mL). To this solution was added 1,2-bis(10,12-tricosadiynoyl)-sn-glycero-3-phosphoethanolamine (436 mg, 500 μmoles) in methylene chloride (5 mL) drop wise using a syringe pump at the rate of 2.5 mL per hour. The starting material had completely disappeared after two hours stirring, as observed by thin layer chromatography. To this reaction was added the integrin antagonist compound (271mg, 550 μmoles) and allowed to stir for 72 hours. The reaction mixture was partitioned between methylene chloride (100 mL) and water (20 mL). The organic layer was separated and washed with brine (10 mL) and then dried over anhydrous sodium sulfate. The solution was filtered to remove sodium sulfate and the solvent was then removed by spin evaporation and the residue was dried under high vacuum over night. The crude product was purified by flash chromatography using $CHCl_3/CH_3OH/H_2O/NH_4OH$ (50/40/5/5) as the solvent to yield 102 mg of the desired product (yield = 13%). ^{1}H NMR: (CDCl3:CD3OD 1:1, 300 MHz, δ ppm) 7.65 (2H, d, Ar-H), 6.75 (2H, d, Ar-H), 0.65–1.05 (116H, overlapping peaks, 2-CH_3 54-CH_2 and 2-CH), 0.8 (6H, s, CH_3). MALDI-MS: $M+H^+$ = 1585.842.

Synthesis of integrin-targeted nanoparticle (ITNP)

The ITNP consists of two lipids with encapsulated rhodamine-B (Figure 1). The first lipid is 1,2-bis(10,12-tricosadiynoyl)-sn-glycero-3-phosphoethanolamine-ethylendiaminetetraacetic acid-integrin antagonist (BisT-PE-EDTA-IA) and the second lipid is the base lipid 1,2-bis(10,12-tricosadiynoyl)-sn-glycero-3-phosphocholine (BisT-PC) lipid. The BisT-PC lipid was purchased from Avanti Polar Lipids. The BisT-PE-EDTA-IA was synthesized from commercially available BisT-PE lipid as described above. Targeting lipid (BisT-PE-EDTA-IA) and the base lipid (BisT-PC, Avanti lipids) were dissolved in a 1:1 mixture of chloroform and methanol and were spin-evaporated to make a thin film. The film was dried under high vacuum over night. This film was hydrated with 10 mM ammonium chloride solution and was gently mixed. The suspension was subjected to 5 consecutive freeze-thaw cycles followed by 5 extrusion cycles through a 100 nm pore size polycarbonate membrane. The extruded particles were then dialyzed against a solution of rhodamine-B for 2 hours. The rhodamine-B loaded ITNPs

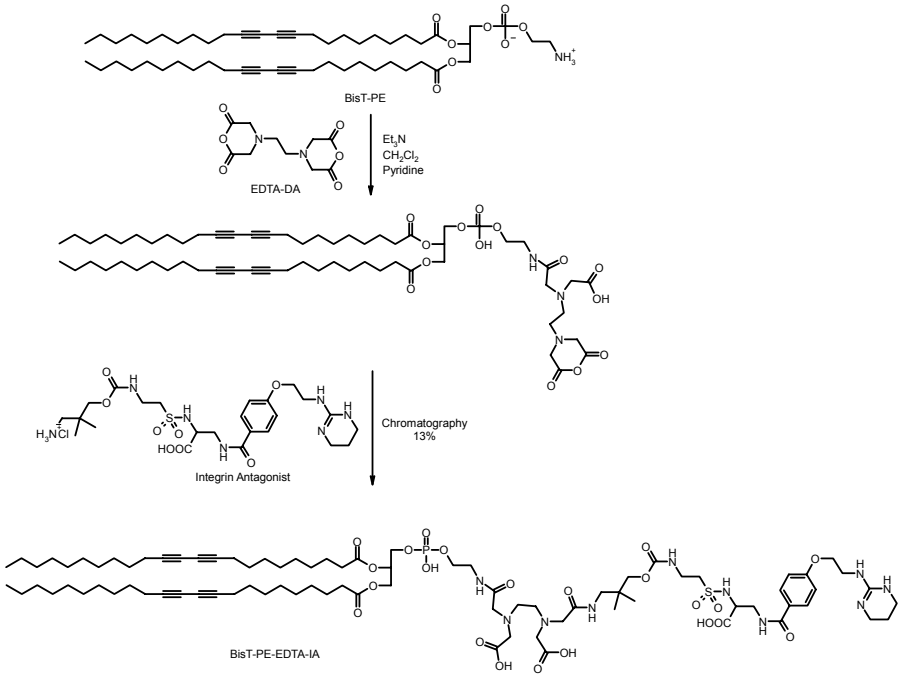

Scheme 1 Schematic illustration for the chemical synthesis of targeting lipid (BisT-PE-EDTA-IA).

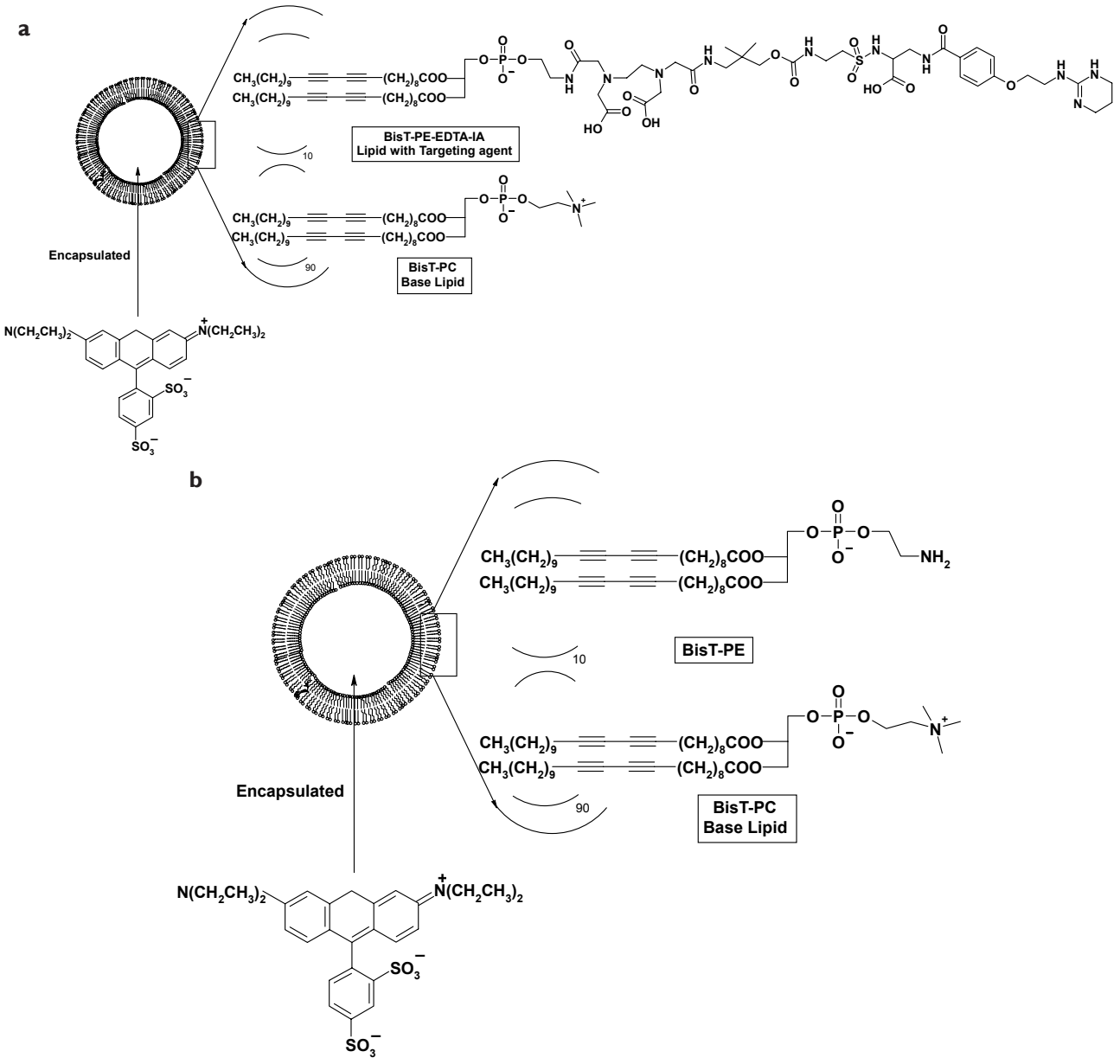

Figure 1 (**a**) Schematic diagram outlining the formation of the ITNPs by self-assembly of the appropriate lipids. The lipid with targeting agent (10 mole%) was combined with base lipid (90 mole%) in a solution of chloroform and methanol (1:1). The mean diameter of the ITNPs was 104.4 ± 3.3 nm, as determined by dynamic light scattering, and the zeta potential was approximately –43.8 mv. The ITNPs were stable for weeks without any observable changes in their physical and biological properties when formulated for use in vivo. (**b**) Schematic diagram outlining the formation of the Control-NPs by self-assembly of the appropriate lipids. The mean diameter of the nanoparticle was 101.2 ± 2.4 nm, as determined by dynamic light scattering, and the zeta potential was approximately –32.6 mv.

were then dialyzed against 10 mM HEPES buffer pH 7.4 for 3 hours. The dialyzed ITNPs were then filtered through 0.2 μ filter into a sterile vial. The size and zeta potential of the ITNPs were determined by dynamic light scattering. The fluorescence spectra was recorded for the rhodamine.

Synthesis of control-NP

The control-NP consists of two lipids with encapsulated rhodamine-B. BisT-PE and BisT-PC lipids (Avanti Polar lipids) were dissolved in a 1:1 mixture of chloroform and methanol and were spin-evaporated to make a thin film. The film was dried under high vacuum over night. This film was hydrated with 10 mM ammonium chloride solution and was gently mixed. The suspension was subjected to 5 consecutive freeze-thaw cycles followed by 5 extrusion cycles through a 100 nm pore size polycarbonate membrane. The extruded particles were then dialyzed against a solution of rhodamine-B for 2 hours. The rhodamine-B loaded NPs were then

dialyzed against 10 mM HEPES buffer pH 7.4 for 3 hours. The dialyzed control-NPs were then filtered through 0.2 μ filter into a sterile vial. The size and zeta potential of the control-NPs were determined by dynamic light scattering.

Transmission electron microscopy of the ITNPs

20 μl of the ITNP was added onto a carbon coated Formvar-film grid. The excess solution was removed by blotting and to this was added 1% phosphotungstic acid solution, pH 7.0. Excess phosphotungstic acid was removed by blotting. The grid surface was then air dried at room temperature. The grid was examined by an electron microscope operated at 75 kV (Hitachi H7000, Tokyo). Digital images were taken by a charge-coupled device camera (Gatan, Pleasanton, CA).

Binding affinity assay

Purified integrin $\alpha_v\beta_3$ protein (Chemicon International, Temecula, CA) was applied to 96-well polystyrene microtiter plates at 0.1 μg/well. After overnight incubation at 4 °C the plates were washed, and then blocked with milk solution (KPL, Inc., Gaithersburg, MD) at room temperature for 2 h. The blocking buffer was removed, and the plates were inoculated in quadruplicate with ITNPs with a typical starting concentration of 1.25 μM. Serial dilutions were prepared in the 96-well plates using multichannel pipette. To each well was added biotinylated vitronectin solution (0.1 μg/well) as standard competitor. The plates were incubated at room temperature for 3 h, washed, and the bound vitronectin was detected using NeutrAvidin-HRP conjugate at 0.01 μg/well (Pierce, Rockford, IL) and LumiGlo chemiluminescent substrate system (KPL, Inc., Gaithersburg, MD). The luminescence was read using a Wallac Counter. The concentration of inhibitor producing 50% inhibition (IC50) of vitronectin binding to $\alpha_v\beta_3$ was calculated based on a curve fitting model (Burnett et al 2005).

Cell uptake assay of the ITNPs

The M21 cells were cultured in RPMI 1640 medium (Biofluids, Gaithersburg, MD) containing 10% fetal calf serum, 2 mM L-glutamine, and penicillin-streptomycin (50 IU ml^{-1} and 50 μg ml^{-1}, respectively, BioSource International; Rockville, MD) at 37 °C with 5% CO_2, and were continuously maintained without over-confluences. Before the experiment, the cells were passaged at 60%–70% confluence two to three times and the cells were loaded to the glass culture chambers for the ITNPs cell uptake assay. Two hours before the cell tracking experiment cells were transferred into fresh medium to ensure the good condition of the cells. The ITNPs were added to the chamber yielding a final concentration of 12 μmol/ml in the presence of 10% fetal bovine serum culture medium for 5 min, 15 min, and 30 min separately to obtain time course of the uptake of ITNPs into the cells. At different time points, the cells in the culture chamber were washed and fixed with 4% Paraformaldehyde-phosphate buffered saline for 20 minutes at RT. After fixing, the cells were washed again and counterstained with a solution of 4′-6-Diamidino-2-phenylindole (DAPI) and observed by the Fluorescence microscopy to obtain the cellular distribution of the ITNPs at different time points.

In vivo/ex vivo studies

A SCC 7, murine squamous cell carcinoma model was used for the in vivo studies. The cells were cultured in RPMI 1640 medium (Biofluids, Gaithersburg, MD) containing 10% fetal calf serum, 2 mM L-glutamine, and penicillin-streptomycin (50 IU ml^{-1} and 50 μg ml^{-1}, respectively, BioSource International, Rockville, MD) at 37 °C with 5% CO_2. The cells were pre-tested as mycoplasm negative (Research Animal Diagnostic Laboratory, University of Missouri, MO). Female C3H mice (6–9 weeks) were purchased from Charles River Laboratories (Gaithersburg, MD) to establish the squamous cell carcinoma mouse model. All animal work was performed according to an approved animal protocol and in compliance with the NIH Clinical Center Animal Care and Use Committee guidelines. Prior to the implantation of the tumor cells, the mice flanks were shaved bilaterally and prepped with isopropyl alcohol. A suspension of SCC-7 cells (1×10^6 cells in 100 μl of PBS) was injected in each of the flanks of each mouse with a 27 G needle. On average, a tumor required 10 days to grow to half centimeter before the mice received the tail-vein injection of Rhodamine-B encapsulated ITNPs. Each mouse received 100 μl of the ITNPs, and after 2 hrs the animal was euthanized. However, 15 minutes before euthanization, the mouse was injected with fluorescein isothiocyante-lectin (FITC-lectin) by tail vein (Hunter et al 2006). The tumor was harvested for cryostat sections. The slides were counterstained with DAPI and the slides were examined with a Zeiss upright microscope using Rhodamine, FITC and DAPI filters to determine the biodistribution of the ITNPs within the cancerous tissues.

Results and discussion

Assembly of integrin-targeted ITNPs

For the construction of the integrin-targeted ITNPs, the critical step is the synthesis of targeting lipid BisT-PE-EDTA-IA as shown in Scheme 1. The IA was synthesized following previously published procedure (Burnett 2005). IA contains a

primary amine functionality for the synthesis of the targeting lipid. EDTA-dianhydride has two reactive anhydrides and can be conjugated to two different amines one on each side by a single pot reaction. The IA and BisT-PE lipid each have one primary amine and by controlled reaction conditions we were able to conjugate them with EDTA-dianhydride. The crude product was purified by column chromatography. The product was characterized by NMR and mass spectrometry. The ITNPs consists of a targeting lipid and a base lipid. These two lipid solutions were mixed together and a film was made by evaporating the solvents. The film was hydrated and after few freeze-thaw cycles, the ITNPs were prepared by extrusion through a polycarbonate membrane. Rhodamine-B was encapsulated inside the particle by ion-exchange process. The particles were purified by dialysis and filtered through 0.2 μm filter into a sterile vial. The mean diameter of the ITNP was 104.4 ± 3.3 nm by dynamic light scattering, the pH was 7.40 and the zeta potential was –43.8 mV. An aliquot of the ITNPs when filtered through 10,000 MW cutoff spin filter, did not show any fluorescence in the filtrate indicating that rhodamine-B was stably encapsulated inside the ITNPs and did not leak out. The ITNPs were stained with phosphotungstic acid at pH 7.0 and examined with Transmission electron microscopy (TEM). The ITNPs appeared as vesicles formed by a single large aqueous cavity surrounded by a thick membrane (Figure 2). The TEM also confirmed the size of ITNP was around 100 nm, in accordance with the measurement by dynamic light scattering.

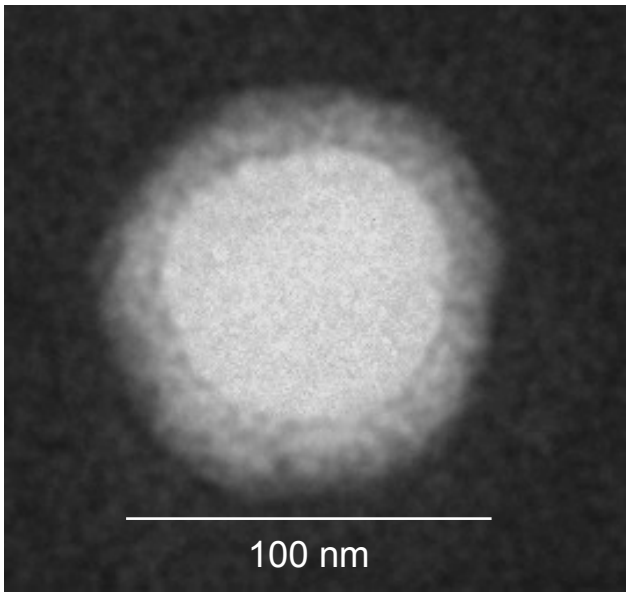

Figure 2 Transmission electron microscopic image of integrin targeted nanoparticles.

Binding affinity and cellular uptake of the ITNPs

The binding affinity of the targeted ITNPs to $\alpha_v\beta_3$ was tested by coating 96 well plates with $\alpha_v\beta_3$. This is a competitive inhibition assay, where the ability of the ITNPs to competitively inhibit the binding of vitronectin to $\alpha_v\beta_3$. We found that ITNPs showed excellent binding affinity to the integrin $\alpha_v\beta_3$ (9.2 nM) (Figure 3). The control nanoparticles did not bind to $\alpha_v\beta_3$ even at very high concentration in the integrin $\alpha_v\beta_3$ plate binding assay (data not shown) which is easy to understand that the bilayer lipids do not have a good binding affinity to the $\alpha_v\beta_3$ protein. Since we did not observe the binding affinity of non-targeted particles to the $\alpha_v\beta_3$ protein, therefore we specifically only observed ITNPs cell uptake and in vivo anagiogenesis targeting as following.

Cell uptake of the ITNPs

When ITNPs were incubated with the M21 cells, it was observed that the ITNPs were accumulated in the cells within minutes and major presented in the cytoplasm of the M21 cells, as observed by fluorescence microscopy (Figure 4). This quick accumulation possibly happens by receptor mediated endocytosis. The uptake of the ITNPs was further investigated by live cell imaging and has been disclosed (Zhang et al 2006).

Tumor angiogenesis targeting

The targeted ITNPs were tail vein injected into C3H mice bearing murine squamous cell carcinoma (SCC-7) tumors to determine the in vivo ability to selectively target angiogenic vessels. Fifteen minutes prior to euthanasia, the animal was tail vein injected with FITC-lectin, which allowed us to observe the functional angiogenic vessels (Hunter 2006) and correlate with the distribution of the ITNPs in the functional angiogenic vessels. The ITNPs were visualized by fluorescence microscopy in the tumor angiogenic vessels which overlapped with the FITC-lectin signal, clearly demonstrating the angiogenesis specific targeting of these ITNPs (Figure 5). Some accumulation was also seen in various other tissues, such as liver and spleen and minimal accumulation was observed in the lung capillary vessels, which warrants further optimization of the ITNPs such as size, charge and lipid composition.

Conclusion

We have synthesized a novel integrin targeted rhodamine-B encapsulated ITNP. This ITNP binds to the integrin $\alpha_v\beta_3$ in

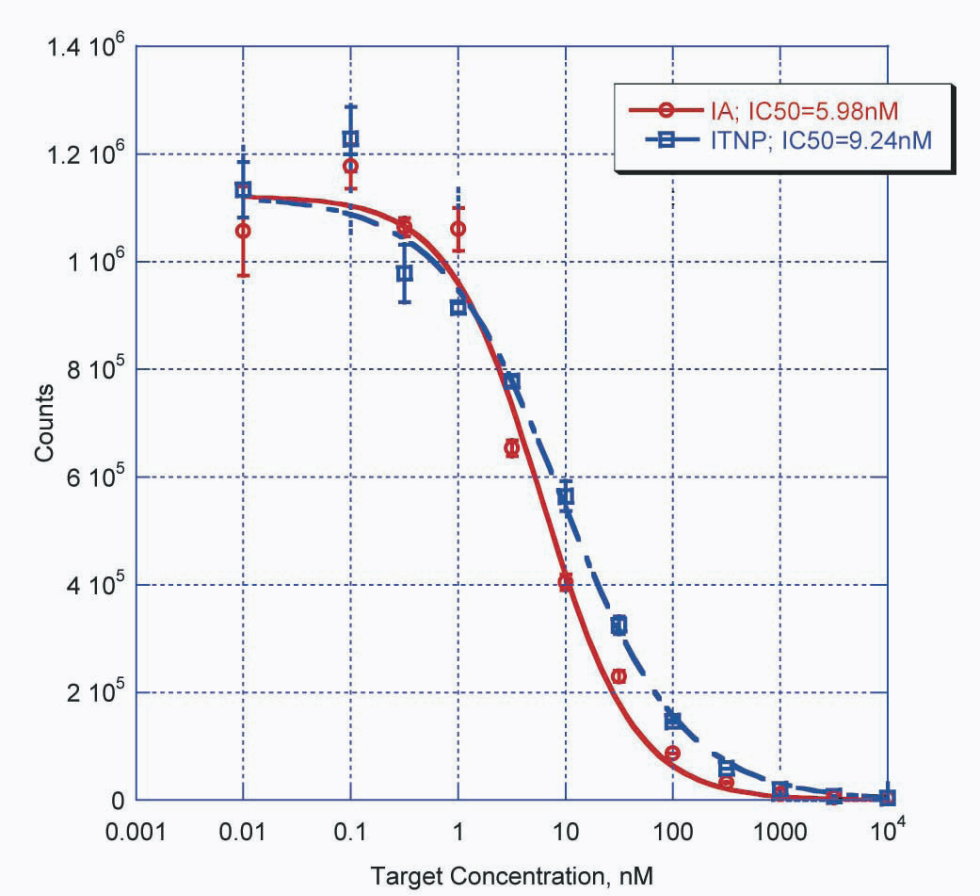

Figure 3 ITNPs binding affinity to the integrin $\alpha_v\beta_3$ protein was quantified by the $\alpha_v\beta_3$ plate binding assay, as in method description. The concentration of inhibitor producing 50% inhibition (IC50) of vitronectin binding to $\alpha_v\beta_3$ was calculated based on a curve fitting model using KaleidaGraph 3.5 (Synergy Software, Reading, PA). ITNPs and targeting agent IA have a closed binding affinity to the $\alpha_v\beta_3$ protein.

the in vitro assay. In vivo the ITNP targets the tumor angiogenic vessels, specially localized within the endothelial cells. Further optimization of this ITNP is feasible by modifying the size, charge and lipid composition. Incorporation of a wide variety of payloads for multi-modality imaging (magnetic resonance imaging, Positron emission tomography and optical imaging) and/or therapy (cytotoxic agent, radionuclide, and anti vascular agents) is in progress.

Acknowledgments

We would like to thank Dr. David Cheresh of Scripps Research Institutes, La Jolla, CA for kindly providing

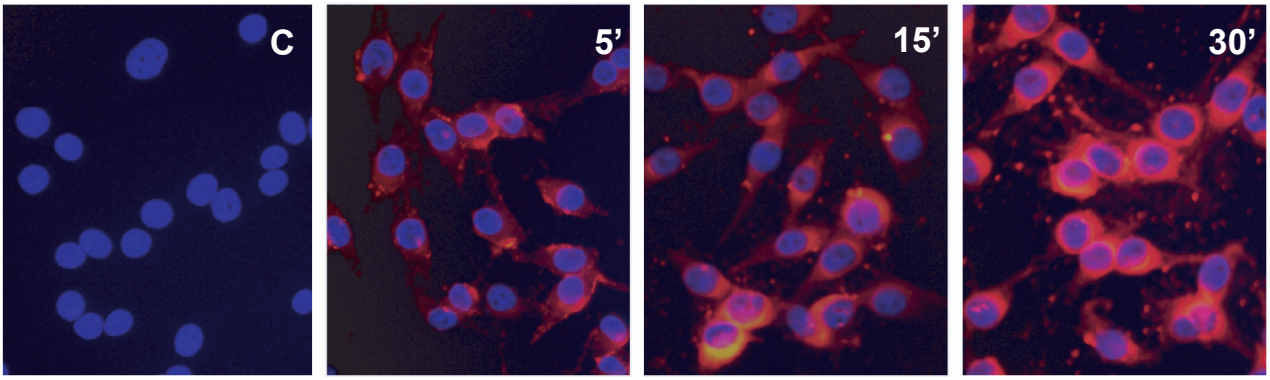

Figure 4 Cellular uptake of the ITNPs by M21 cells in vitro. The ITNPs were added to the chamber yielding a final concentration of 12 μmol/ml. After 5, 15, and 30 minutes of incubation, the cells were washed, stained with DAPI and observed by fluorescence microscopy.

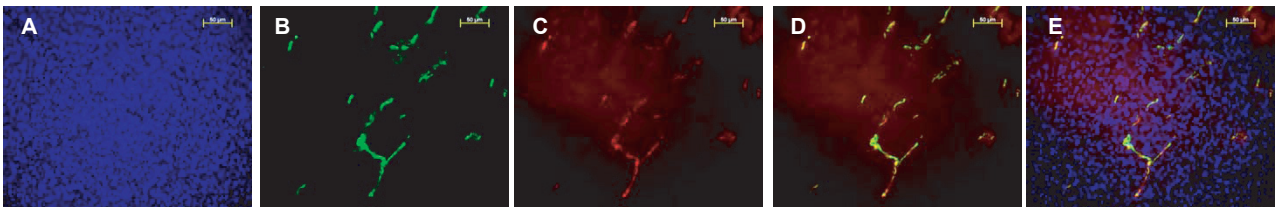

Figure 5 Angiogenic vessel targeting by the ITNPs. A: SCC-7 Cell nucleus stained by DAPI, B: Functional angiogenic vessels stained by injected FITC-Lectin, C: angiogenic vessels targeting by ITNPs observed by Rhodamine, D: Merge signals of the ITNPs targeted vessels and functional angiogenic vessels labeled by Lectin, E: Merge signals of the ITNPs targeted vessels, functional angiogenic vessels labeled by Lectin, and cell nuclear staining by DAPI. (scale bar = 50 um).

the M21 cells. The SCC 7 cells were kindly provided by Dr. Anastasia Sowers, Radiation Oncology Branch, National Cancer Institute, Bethesda, MD. We also would like to thank Dr. Kunio Nagashima of National Cancer Institute for his help with the TEM. Special thanks go to Dr. Dale Kiesewetter and Dr. L. Henry Bryant for their help with this manuscript. The intramural research program of the NIH Clinical Center supported this work.

References

Burnett CA, Xie J, Quijano J, et al. 2005. Synthesis, in vitro, and in vivo characterization of an integrin alpha(v)beta(3)-targeted molecular probe for optical imaging of tumor. *Bioorg Med Chem*, 13:3763–71.

Duggan ME, Duong LT, Fisher JE, et al. 2000. Nonpeptide alpha(v)beta(3) antagonists. 1. Transformation of a potent, integrin-selective alpha(IIb)beta(3) antagonist into a potent alpha(v)beta(3) antagonist. *J Med Chem*, 43:3736–45.

Eliceiri BP, Cheresh DA. 2000. Role of alpha v integrins during angiogenesis. *Cancer Journal*, 6:S245–9.

Gutheil JC, Campbell TN, Pierce PR, et al. 2000. Targeted antiangiogenic therapy for cancer using Vitaxin: a humanized monoclonal antibody to the integrin $\alpha_v\beta_3$. *Can Res*, 61:1781–5.

Hood JD, Bednarski M, Frausto R, et al. 2002. Tumor regression by targeted gene delivery to the neovasculature. *Science*, 296:2404–7.

Hunter F, Xie J, Trimble C, et al. 2006. Rhodamine-RCA in vivo labeling guided laser capture microdissection of cancer functional angiogenic vessels in a murine squamous cell carcinoma mouse model. *Mol Can*, 5:1–11.

Lim EH, Danthi SN, Bednarski M, et al. 2005. A review: Integrin avb3-targeted molecular imaging and therapy in angiogenesis. *Nanomedicine: Nanotech Biol Med*, 1:110–14.

Raguse JD, Gath HJ, Bier J, et al. 2004. Cilengitide (EMD 121974) arrests the growth of a heavily pretreated highly vascularised head and neck tumour. *Oral Oncol*, 40:228–30.

Ruoslahti E. 2002. Specialization of tumour vasculature. *Nat Rev Cancer*, 2:83–90.

Storrs RW, Tropper FD, Li HY, et al. 1995. Paramagnetic polymerized liposomes: synthesis, characterization, and applications for magnetic resonance imaging. *J Am Chem Soc*, 28:7301–6.

Sipkins DA, Cheresh DA, Kazemi MR, et al. 1998. Detection of tumor angiogenesis in vivo by alphaVbeta3-targeted magnetic resonance imaging. *Nat Med*, 4:623–6.

Taga T, Suzuki A, Gonzalez-Gomez I, et al. 2002. Integrin antagonist EMD 121974 induces apoptosis in brain tumor cells growing on vitronectin and tenascin. *Int J Cancer*, 98:690–7.

Tucker GC. 2006. Integrins: molecular targets in cancer therpay. *Cur Oncol Reports*, 8:96–103.

Winter PM, Morawski AM, Caruthers SD, et al. 2003. Molecular imaging of angiogenesis in early-stage atherosclerosis with $\alpha_v\beta_3$-integrin-targeted nanoparticles. *Circulation*, 108:2270–4.

Zhang T, Danthi SN, Xie J, et al. 2006. Live cell imaging of the endocytosis and the intracellular trafficking of multifunctional lipid nanoparticles. *Proc SPIE NanoBiophotonics Biomedical Appln*, 3:6095.